Adaptive finite-time 6-DOF control of satellite proximation with non-cooperative target [⋆]

Zhi Gao [*] Zhihao Zhu [**] Yu Guo [***]

[*] *College of Information Engineering, Yancheng Institute of Technology, Yancheng, China (e-mail: zgao@ycit.edu.cn).*
[**] *School of Electrical Engineering, Yancheng Institute of Technology, Yancheng, China (e-mail: zhzhu@ycit.edu.cn)*
[***] *School of Automation, Nanjing University of Science and Technology, Nanjing, China, (e-mail: guoyu@njust.edu.cn)*

Abstract: For satellite proximation with non-cooperative target, uncertainties and state-dependent disturbances, this paper is concerned with an adaptive finite-time (AFT) six degrees of freedom (6-DOF) control. First, to ensure the accurate relative maneuvers, the 6-DOF coupled system of the satellite is constructed. Then to realize high precision proximity control, an AFT 6-DOF coupled control strategy with a self-adjustment function is developed. The self-adjustment function is exploited to improve the convergence performance. Coupled adaptive update laws are developed to estimate the unknown mass, inertia and disturbance. Comparisons of simulation are provided to discuss the properties of the AFT 6-DOF control.

Keywords: Non-cooperative target, Uncertainties and disturbances, 6-DOF, Finite-time control, Self-adjustment function.

1. INTRODUCTION

Satellite proximity operations play the role of a critical skill for numerous space missions, such as satellite navigation, junk cleanup, maintaining, space target capturing, repairing, fueling and space exploration (Oestreich et al. (2021); Zhao and Duan (2023)). Proximity operations require precise 6-DOF control technology which include attitude and position control, it is crucial to space mission success. The naturally coupled characteristics between attitude and position are strong. Traditionally, the control schemes of attitude (Lee and Gallucci (2023); Zhu et al. (2020)) and of position (Wang et al. (2021); Zhuang et al. (2021)) are developed independently, it may result the satisfactory control performance cannot be realized. The 6-DOF control with considering of the strong couplings has become a severe challenge.

Various results about 6-DOF control has been proposed in recent years. Artificial potential function based 6-DOF approach strategy was presented to simultaneously control the position and attitude (Wang et al. (2022)). A pose tracking control structure was constructed for satellite regardless of inertia and mass uncertainties, employing the prescribed performance control methodology (Shao et al. (2020)). A nonlinear feedback 6-DOF controller was designed with a disturbance observer (Li et al. (2018)). In practical applications, the uncertainty and disturbance may decrease the system stability, the aforementioned works (Wang et al. (2022); Shao et al. (2020); Li et al. (2018)) only consider one aspect affect. A 6-DOF controller based on backstepping was developed for satellite proximation (Zhu et al. (2024)). Based on neural network, a controller was constructed with taking into account uncertainty and disturbance, where the parameter uncertainty and disturbance are bounded (Wang et al. (2020)). For proximity operations with the disturbance and uncertainty, an 6-DOF sliding mode control which is essentially PD-type $H\infty$ control was investigated (Kasiri and Fani Saberi (2023)). The 6-DOF control methods (Zhu et al. (2024); Wang et al. (2020); Kasiri and Fani Saberi (2023)) can only accomplish bounded or asymptotic stability.

For the sake of faster convergence and better robustness for satellite, the finite-time (FT) 6-DOF control has attracted widespread interest. A neural network-based prescribed performance appointed-time control algorithm was constructed to satisfy the requirements of the relative position and attitude with system uncertainty and external disturbance (Zhang et al. (2022)). A FT relative motion controller by employing sliding mode was built for regulate the relative motion (Liu et al. (2021)). A FT controller was presented to regulate the satellite to track setting states with unknown disturbance (Chen et al. (2023)). It is well known that the disturbance is time-varying and affected by the aerodynamics, namely, the disturbance is state-dependent. In aforesaid works (Zhang et al. (2022); Liu et al. (2021); Chen et al. (2023)), the bounds of the disturbances were considered to be unknown constants. Moreover, the system (Zhang et al. (2022); Liu et al. (2021)) of the modified Rodriguez parameters model exists the singular point. As far as I known, the AFT 6-DOF con-

[⋆] This research is funded by the National Natural Science Foundation of China (Grant Nos. 61973167 and 62033011), Cooperative education project of the Ministry of Education (22097110113736).

trol problem for chaser to approach a non-cooperative target with mass uncertainty, inertia uncertainty and state-dependent disturbance still be an open problem.

Due to the lack of a solution of the open problem, an AFT 6-DOF coupled control algorithm is proposed with consideration of the non-cooperative target, system couplings, mass uncertainty, inertia uncertainty and unknown time-varying state-dependent disturbance. This study contains the following contributions:

(1) Unlike the works (Zhang et al. (2022); Liu et al. (2021)), a new nonsingular relative motion system model is constructed, which can avoid the geometric singularity.
(2) Compared to the above mentioned works (Zhang et al. (2022); Liu et al. (2021); Chen et al. (2023)), a coupled AFT 6-DOF tracking controller with a self-adjustment function is constructed to accurately restrain the influence of the unknown uncertainties and the unknown time-varying disturbances related to states. Furthermore, the proposed self-adjustment function can enhance the convergence performance.
(3) In contrary to the aforementioned works (Zhu et al. (2024); Wang et al. (2020); Kasiri and Fani Saberi (2023)), the proposed coupled AFT 6-DOF tracking controller can implement the finite time stability with faster convergence and better robustness.

2. PRELIMINARIES

Notations. For vector $b = [b_1, b_2, \cdots, b_n]^{\mathrm{T}} \in R^n$ and real number α, $\|b\|$ represents the 2-norm of b, $L(b) = \begin{bmatrix} b_1 & 0 & 0 & 0 & b_3 & b_2 \\ 0 & b_2 & 0 & b_3 & 0 & b_1 \\ 0 & 0 & b_3 & b_2 & b_1 & 0 \end{bmatrix}$, $b^\alpha = [b_1^\alpha, b_2^\alpha, \cdots, b_n^\alpha]^{\mathrm{T}}$ and $\mathrm{sig}^\alpha(b) = [\mathrm{sign}(b_1)|b_1|^\alpha, \mathrm{sign}(b_2)|b_2|^\alpha, \cdots, \mathrm{sign}(b_n)|b_n|^\alpha]^{\mathrm{T}}$ with $\mathrm{sign}(b_i)$ is the standard sign function. For $a, b \in R^{3\times 1}$ and skew-symmetric matrix operator $^\times$, $a^\times a = 0$, $\|a^\times\| = \|a\|$ and $a^\times b = -b^\times a$. $0_m = 0^{m\times m}$, $I_m = 1^{m\times m}$ and $0_{m\times n} = 0^{m\times n}$.

2.1 Control objective

The finite-time 6-DOF control puzzler that the satellite proximation operations with non-cooperative target, mass and inertia uncertainties and state-dependent disturbances is investigated. The control objective is to achieve the chaser attitude and the chaser mass center synchronized with the target attitude and the fixed position P respectively within finite time for Fig. 1.

2.2 System model

The coupled 6-DOF system model are given as (Zhu et al. (2024))

$$\dot r = v - \omega^\times r \tag{1}$$

$$\begin{bmatrix} \dot q \\ \dot\varsigma \end{bmatrix} = \begin{bmatrix} \frac{1}{2}(q^\times + \varsigma I_3)\omega \\ -\frac{1}{2} q^{\mathrm{T}}\omega \end{bmatrix} \tag{2}$$

$$m\dot v = -m\omega^\times v + f + d_f \tag{3}$$

$$J\dot\omega = -\omega^\times J\omega + \tau + d_\tau \tag{4}$$

where $r \in R^3$, $[q^{\mathrm{T}}, \varsigma]^{\mathrm{T}} \in R^4$, $v \in R^3$ and $\omega \in R^3$ represent the chaser position, attitude, linear and angular

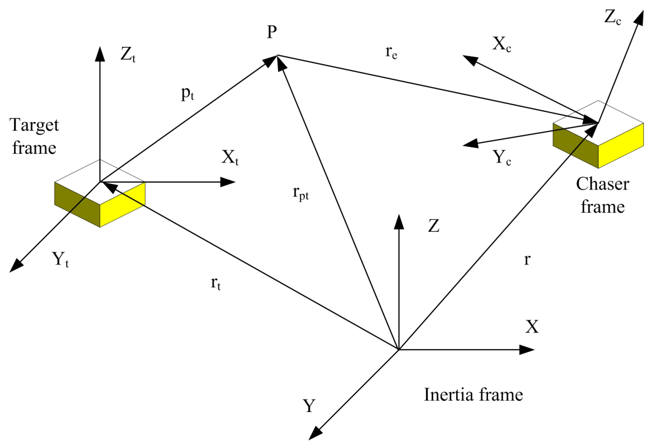

Fig. 1. Space frame and vector

velocities with $q^{\mathrm{T}} q + \varsigma^2 = 1$, respectively. $m \in R$ and $J = \begin{bmatrix} J_{11} & J_{12} & J_{13} \\ J_{12} & J_{22} & J_{23} \\ J_{13} & J_{23} & J_{33} \end{bmatrix}$ are the mass and inertia matrix. $f \in R^3$, $\tau \in R^3$, $d_f \in R^3$ and $d_\tau \in R^3$ denote the force and torque with the physical actuator and the external disturbance, respectively.

The model of the target is

$$\dot r_t = v_t - \omega_t^\times r_t \tag{5}$$

$$\begin{bmatrix} \dot q_t \\ \dot\varsigma_t \end{bmatrix} = \begin{bmatrix} \frac{1}{2}(q_t^\times + \varsigma_t I_3)\omega_t \\ -\frac{1}{2} q_t^{\mathrm{T}}\omega_t \end{bmatrix} \tag{6}$$

$$m_t \dot v_t = -m_t \omega_t^\times v_t \tag{7}$$

$$J_t \dot\omega_t = -\omega_t^\times J_t \omega_t \tag{8}$$

Furthermore, the vectors

$$r_{pt} = p_t + r_t \tag{9}$$

$$v_{pt} = \omega_t^\times p_t + v_t \tag{10}$$

where $p_t \in R^3$ is a constant vector. Then,

$$\dot r_{pt} = v_{pt} - \omega_t r_{pt} \tag{11}$$

$$\dot v_{pt} = \dot\omega_t^\times p_t + \dot v_t \tag{12}$$

The response error are described as

$$\begin{bmatrix} q_e \\ \varsigma_e \end{bmatrix} = \begin{bmatrix} \varsigma_t q - \varsigma q_t - q_t^\times q \\ \varsigma_t \varsigma + q_t^{\mathrm{T}} q \end{bmatrix} \tag{13}$$

$$r_e = r - N r_{pt} \tag{14}$$

$$\omega_e = \omega - N\omega_t \tag{15}$$

$$v_e = v - N v_{pt} \tag{16}$$

where $q_e^{\mathrm{T}} q_e + \varsigma_e^2 = 1$, $N = (\varsigma_e^2 - q_e^{\mathrm{T}} q_e) I_3 + 2 q_e q_e^{\mathrm{T}} - 2\varsigma_e q_e^\times$ with $\|N\| = 1$.

In virtue of $N\sigma^\times = (N\sigma)^\times N$ for any $\sigma = [\sigma_1, \sigma_2, \sigma_3]^{\mathrm{T}}$ and $\dot N = -\omega_e^\times N$, one has

$$\begin{aligned} N\dot v_{pt} = &-(\omega - \omega_e)^\times v + (\omega - \omega_e)^\times v_e \\ &+ (\omega - \omega_e)^\times (\omega - \omega_e)^\times N p_t - N p_t^\times \dot\omega_t \end{aligned} \tag{17}$$

$$\begin{aligned} \dot\omega_t &= -J_t^{-1} \omega_t^\times J_t \omega_t \\ &= -J_t^{-1} (N^{\mathrm{T}}(\omega - \omega_e))^\times J_t N^{\mathrm{T}} (\omega - \omega_e) \end{aligned} \tag{18}$$

then, the relative motion system is modeled as

$$\begin{bmatrix} \dot q_e \\ \dot\varsigma_e \end{bmatrix} = \frac{1}{2} \begin{bmatrix} q_e^\times + \varsigma_e I_3 \\ -q_e^{\mathrm{T}} \end{bmatrix} \omega_e \tag{19}$$

$$\dot{r}_e = v_e - \omega^{\times} r_e \tag{20}$$

$$\begin{aligned} J\dot{\omega}_e = & -\omega^{\times} J\omega - J\omega^{\times}\omega_e \\ & + JNJ_t^{-1}(N^{\mathrm{T}}(\omega - \omega_e))^{\times} J_t N^{\mathrm{T}}(\omega - \omega_e) \\ & + \tau + d_\tau \end{aligned} \tag{21}$$

$$\begin{aligned} m\dot{v}_e = & -m\omega^{\times} v_e - m(\omega - \omega_e)^{\times}(\omega - \omega_e)^{\times} N p_t \\ & - mNp_t^{\times}(\omega - \omega_e)^{\times} J_t N^{\mathrm{T}}(\omega - \omega_e) + f + d_f \end{aligned} \tag{22}$$

Assumption 1 (Zhu et al. (2024)) J and J_t are uncertain constant matrices, m and m_t are uncertain constants. The state-dependant d_τ and $d_f$satisfy $\|d_\tau\| \le c_1(1 + \|\omega\|^2)$ and $\|d_f\| \le c_2(1 + \|v\|^2)$ with unknown constants c_1 and c_2.

Assumption 2 (Sun and Huo (2014)) $\{r, q, \varsigma, v, \omega\}$ and $\{r_e, q_e, \varsigma_e, v_e, \omega_e\}$ can be directly measured by the chaser. Moreover, the target satellite is non-cooperative, in other words, $\{r_t, q_t, \varsigma_t, v_t, \omega_t\}$ can not be obtained.

Lemma 1 (Hardy et al. (1952)) For any constants x_i and $0 < \alpha \le 1$, $(\sum_{i=1}^{n} |x_i|)^\alpha \le \sum_{i=1}^{n} |x_i|^\alpha \le n^{1-\alpha}(\sum_{i=1}^{n} |x_i|)^\alpha$.

Lemma 2 (POLYCARPOU and IOANNOU (1996)) For any $\beta > 0$ and $x \in R$, there exist $0 \le |x| - x\tanh(\beta x) \le \dfrac{\phi}{\beta}$, where $\phi = e^{-(\phi+1)}$, namely, $\phi = 0.2785$.

Lemma 3 (Zhu et al. (2011)) Suppose that the Lyapunov function $V(x)$, constants $l > 0$, $0 < \alpha < 1$ and $0 < \delta < \infty$ satisfy $\dot{V}(x) \le -lV^\alpha(x) + \delta$. Then, the closed-loop system is practical finite time stable and the convergence region is $V(x(T)) \le \dfrac{\delta}{(1-\kappa)l}$ with reach time $T \le \dfrac{V(x(0))}{l\kappa(1-\alpha)}$, where $x(0)$ is the initial value and real number κ satisfies $0 < \kappa < 1$.

3. AFT 6-DOF CONTROLLER DESIGN

An AFT 6-DOF proximation control problem with noncooperative target will be carried out as shown in Fig. 2.

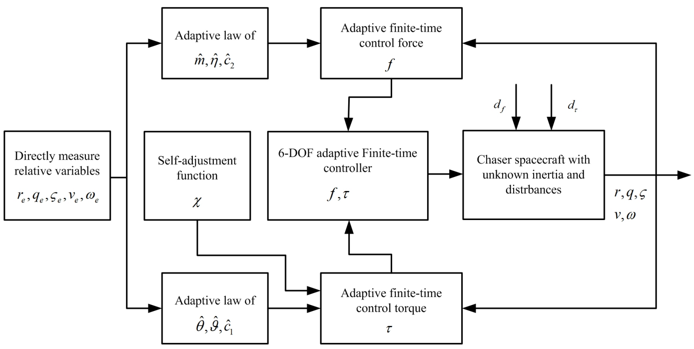

Fig. 2. Control strategy

The AFT 6-DOF controller is designed as

$$\begin{aligned} \tau = & -k_1(q_e^{\times} + \varsigma_e I_3)^{\mathrm{T}} q_e - \chi k_2 \mathrm{sig}^\alpha(\omega_e) - Y\hat{\theta} \\ & - \hat{\vartheta}\|\omega - \omega_e\|^2 \tanh(\beta_2 \omega_e) - \frac{\hat{c}_1 \omega_e \psi_1}{\|\omega_e\| + \varepsilon_3} \end{aligned} \tag{23}$$

$$\begin{aligned} f = & -\rho_1 r_e - k_3 \mathrm{sig}^\alpha(v_e) - k_4 v_e \\ & + \hat{m}(\omega - \omega_e)^{\times}(\omega - \omega_e)^{\times} N p_t \\ & - \hat{\eta}\|p_t\|\|\omega - \omega_e\|^2 \tanh(\beta_5 v_e) - \frac{\hat{c}_2 v_e \psi_2}{\|v_e\| + \varepsilon_7} \end{aligned} \tag{24}$$

where k_1, k_2, k_3, k_4, $0 < \alpha < 1$, ρ_1, β_2 and β_5 are positive constants, $\chi = 1 + \sigma_1 - e^{\sigma_2 t}$ is a self-adjustment function with two positive constants $\sigma_1 < 1$ and σ_2, $Y = -\omega^{\times} L(\omega) - L(\omega^{\times}\omega_e)$, $\hat{\theta}$, $\hat{m}$, $\hat{c}_1$, $\hat{c}_2$, $\hat{\vartheta}$ and $\hat{\eta}$ are the estimate of $\theta = [J_{11}, J_{22}, J_{33}, J_{32}, J_{31}, J_{21}]^{\mathrm{T}}$, m, c_1, c_2, $\vartheta = \|J\|\|J_t^{-1}\|\|J_t\|$ and $\eta = m\|J_t\|$, respectively, $\psi_1 = 1 + \|\omega\|^2$, $\psi_2 = 1 + \|v\|^2$, ε_3 and ε_7 will be introduced in the design of adaptive update laws which are

$$\dot{\hat{\theta}} = b_1(Y^{\mathrm{T}}\omega_e - b_2\hat{\theta}) \tag{25}$$

$$\dot{\hat{m}} = -\delta_1 v_e^{\mathrm{T}}(\omega - \omega_e)^{\times}(\omega - \omega_e)^{\times} N p_t - \delta_1\delta_2\hat{m} \tag{26}$$

$$\dot{\hat{\vartheta}} = \beta_1(\|\omega - \omega_e\|^2 \omega_e^{\mathrm{T}} \tanh(\beta_2\omega_e) - \beta_3\hat{\vartheta}) \tag{27}$$

$$\dot{\hat{\eta}} = \beta_4(\|p_t\|\|\omega - \omega_e\|^2 v_e^{\mathrm{T}} \tanh(\beta_5 v_e) - \beta_6\hat{\eta}) \tag{28}$$

$$\dot{\hat{c}}_1 = -\varepsilon_1\hat{c}_1 + \frac{\varepsilon_2\|\omega_e\|^2\psi_1}{\|\omega_e\| + \varepsilon_3}, \varepsilon_3 = \frac{\varepsilon_4}{1 + \psi_1} \tag{29}$$

$$\dot{\hat{c}}_2 = -\varepsilon_5\hat{c}_2 + \frac{\varepsilon_6\|v_e\|^2\psi_2}{\|v_e\| + \varepsilon_7}, \varepsilon_7 = \frac{\varepsilon_8}{1 + \psi_2} \tag{30}$$

where $b_1 > 0$ and $b_2 > 0$ with $b_1 b_2 \ge 1$, $\delta_1 > 0$, $\delta_2 > 0$, $\delta_1\delta_2 \ge 1$, $\beta_1 > 0$, $\beta_3 > 0$, $\beta_1\beta_3 \ge 1$, $\beta_4 > 0$, $\beta_6 > 0$, $\beta_4\beta_6 \ge 1$, $\varepsilon_1 \ge 1$, $\varepsilon_2 > 0$, $\varepsilon_4 > 0$, $\varepsilon_5 \ge 1$, $\varepsilon_6 > 0$, $\varepsilon_8 > 0$.

Remark 1 Due to $t \ge 0$, χ is a self-adjustment function with $\sigma_1 \le \chi \le 1 + \sigma_1$. According to Eqs.(21) and (23), χ can reduce the amplitude of ω_e and further enhance the convergence procedure of the ω_e, q_e, v_e and r_e.

Theorem 1. For the coupled 6-DOF system (19)-(22) under Assumptions 1 and 2, the system will be practical finite time stable under AFT 6-DOF controller (23)-(24).

Proof. Defining estimate errors $\tilde{\theta} = \hat{\theta} - \theta$, $\tilde{m} = \hat{m} - m$, $\tilde{\vartheta} = \hat{\vartheta} - \vartheta$, $\tilde{\eta} = \hat{\eta} - \eta$, $\tilde{c}_1 = \hat{c}_1 - c_1$ and $\tilde{c}_2 = \hat{c}_2 - c_2$, a Lyapunov function is

$$\begin{aligned} V = & \frac{1}{2}\omega_e^{\mathrm{T}} J\omega_e + k_1 q_e^{\mathrm{T}} q_e + \frac{1}{2} v_e^{\mathrm{T}} m v_e + \frac{\rho_1}{2} r_e^{\mathrm{T}} r_e \\ & + \frac{1}{2b_1}\tilde{\theta}^{\mathrm{T}}\tilde{\theta} + \frac{1}{2\delta_1}\tilde{m}^2 + \frac{1}{2\beta_1}\tilde{\vartheta}^2 + \frac{1}{2\beta_4}\tilde{\eta}^2 \\ & + \frac{1}{2\varepsilon_2}\tilde{c}_1^2 + \frac{1}{2\varepsilon_6}\tilde{c}_2^2 \end{aligned} \tag{31}$$

Let

$$V = V_1 + V_2 \tag{32}$$

with

$$V_1 = \frac{1}{2}\omega_e^{\mathrm{T}} J\omega_e + k_1 q_e^{\mathrm{T}} q_e + \frac{1}{2b_1}\tilde{\theta}^{\mathrm{T}}\tilde{\theta} + \frac{1}{2\beta_1}\tilde{\vartheta}^2 + \frac{1}{2\varepsilon_2}\tilde{c}_1^2 \tag{33}$$

$$V_2 = \frac{1}{2} v_e^{\mathrm{T}} m v_e + \frac{\rho_1}{2} r_e^{\mathrm{T}} r_e + \frac{1}{2\delta_1}\tilde{m}^2 + \frac{1}{2\beta_4}\tilde{\eta}^2 + \frac{1}{2\varepsilon_6}\tilde{c}_2^2 \tag{34}$$

Step 1. Analyzing the derivative of V_1.

From (19), (21), (25), (27) and (29), one has

$$\begin{aligned} \dot{V}_1 = & \omega_e^{\mathrm{T}} J\dot{\omega}_e + 2k_1 q_e^{\mathrm{T}}\dot{q}_e + \frac{1}{b_1}\tilde{\theta}^{\mathrm{T}}\dot{\hat{\theta}} + \frac{1}{\beta_1}\tilde{\vartheta}\dot{\hat{\vartheta}} + \frac{1}{\varepsilon_2}\tilde{c}_1\dot{\hat{c}}_1 \\ = & \omega_e^{\mathrm{T}}(-\omega^{\times} J\omega - J\omega^{\times}\omega_e \\ & + JNJ_t^{-1}(N^{\mathrm{T}}(\omega - \omega_e))^{\times} J_t N^{\mathrm{T}}(\omega - \omega_e) + \tau \\ & + d_\tau) + k_1 q_e^{\mathrm{T}}(q_e^{\times} + \varsigma_e I_3)\omega_e + \tilde{\theta}^{\mathrm{T}}(Y^{\mathrm{T}}\omega_e - b_2\hat{\theta}) \\ & + \tilde{\vartheta}(\|\omega - \omega_e\|^2 \omega_e^{\mathrm{T}} \tanh(\beta_2\omega_e) - \beta_3\hat{\vartheta}) \\ & + \frac{1}{\varepsilon_2}\tilde{c}_1(-\varepsilon_1\hat{c}_1 + \frac{\varepsilon_2\|\omega_e\|^2\psi_1}{\|\omega_e\| + \varepsilon_3}) \end{aligned} \tag{35}$$

Because

$$J\omega = L(\omega)\theta \tag{36}$$

$$J\omega^{\times}\omega_e = L(\omega^{\times}\omega_e)\theta \tag{37}$$

Eq. (35) can be expressed as

$$\begin{aligned}\dot{V}_1 &= \omega_e^{\mathrm{T}}(-\omega^{\times}L(\omega)\theta - L(\omega^{\times}\omega_e)\theta \\ &\quad + JNJ_t^{-1}(N^{\mathrm{T}}(\omega-\omega_e))^{\times}J_tN^{\mathrm{T}}(\omega-\omega_e) \\ &\quad + \tau + d_\tau) + k_1 q_e^{\mathrm{T}}(q_e^{\times} + \varsigma_e I_3)\omega_e + \tilde{\theta}^{\mathrm{T}}Y^{\mathrm{T}}\omega_e \\ &\quad - b_2\tilde{\theta}^{\mathrm{T}}\hat{\theta} + \tilde{\vartheta}\|\omega-\omega_e\|^2\omega_e^{\mathrm{T}}\tanh(\beta_2\omega_e) \\ &\quad - \beta_3\tilde{\vartheta}\hat{\vartheta} - \frac{\varepsilon_1}{\varepsilon_2}\tilde{c}_1\hat{c}_1 + \frac{\tilde{c}_1\|\omega_e\|^2\psi_1}{\|\omega_e\|+\varepsilon_3} \\ &\le \omega_e^{\mathrm{T}}(-\omega^{\times}L(\omega)\theta - L(\omega^{\times}\omega_e)\theta + \tau + d_\tau) \\ &\quad + k_1 q_e^{\mathrm{T}}(q_e^{\times} + \varsigma_e I_3)\omega_e \\ &\quad + \|J\|\|J_t^{-1}\|\|J_t\|\|N\|^3\|\omega-\omega_e\|^2\|\omega_e\| + \tilde{\theta}^{\mathrm{T}}Y^{\mathrm{T}}\omega_e \\ &\quad - b_2\tilde{\theta}^{\mathrm{T}}\hat{\theta} + \tilde{\vartheta}\|\omega-\omega_e\|^2\omega_e^{\mathrm{T}}\tanh(\beta_2\omega_e) \\ &\quad - \beta_3\tilde{\vartheta}\hat{\vartheta} - \frac{\varepsilon_1}{\varepsilon_2}\tilde{c}_1\hat{c}_1 + \frac{\tilde{c}_1\|\omega_e\|^2\psi_1}{\|\omega_e\|+\varepsilon_3}\end{aligned} \tag{38}$$

Under Assumption 1 and 2, using $Y = -\omega^{\times}L(\omega) - L(\omega^{\times}\omega_e)$, $\vartheta = \|J\|\|J_t^{-1}\|\|J_t\|$ and $\|N\| = 1$ yield

$$\begin{aligned}\dot{V}_1 &\le \omega_e^{\mathrm{T}}Y\theta + \omega_e^{\mathrm{T}}\tau + \|\omega_e\|c_1\psi_1 + \vartheta\|\omega-\omega_e\|^2\|\omega_e\| \\ &\quad + k_1 q_e^{\mathrm{T}}(q_e^{\times} + \varsigma_e I_3)\omega_e + \tilde{\theta}^{\mathrm{T}}Y^{\mathrm{T}}\omega_e - b_2\tilde{\theta}^{\mathrm{T}}\hat{\theta} \\ &\quad + \tilde{\vartheta}\|\omega-\omega_e\|^2\omega_e^{\mathrm{T}}\tanh(\beta_2\omega_e) \\ &\quad - \beta_3\tilde{\vartheta}\hat{\vartheta} - \frac{\varepsilon_1}{\varepsilon_2}\tilde{c}_1\hat{c}_1 + \frac{\tilde{c}_1\|\omega_e\|^2\psi_1}{\|\omega_e\|+\varepsilon_3}\end{aligned} \tag{39}$$

Applying controller (23), Eq.(39) can be rewritten as

$$\begin{aligned}\dot{V}_1 &\le \omega_e^{\mathrm{T}}(-k_1(q_e^{\times} + \varsigma_e I_3)^{\mathrm{T}}q_e - \chi k_2\mathrm{sig}^{\alpha}(\omega_e) - Y\hat{\theta} \\ &\quad - \hat{\vartheta}\|\omega-\omega_e\|^2\tanh(\beta_2\omega_e) - \frac{\hat{c}_1\omega_e\psi_1}{\|\omega_e\|+\varepsilon_3}) \\ &\quad + \omega_e^{\mathrm{T}}Y\theta + \|\omega_e\|c_1\psi_1 + \vartheta\|\omega-\omega_e\|^2\|\omega_e\| \\ &\quad + k_1 q_e^{\mathrm{T}}(q_e^{\times} + \varsigma_e I_3)\omega_e + \tilde{\theta}^{\mathrm{T}}Y^{\mathrm{T}}\omega_e - b_2\tilde{\theta}^{\mathrm{T}}\hat{\theta} \\ &\quad + \tilde{\vartheta}\|\omega-\omega_e\|^2\omega_e^{\mathrm{T}}\tanh(\beta_2\omega_e) - \beta_3\tilde{\vartheta}\hat{\vartheta} \\ &\quad - \frac{\varepsilon_1}{\varepsilon_2}\tilde{c}_1\hat{c}_1 + \frac{\tilde{c}_1\|\omega_e\|^2\psi_1}{\|\omega_e\|+\varepsilon_3}\end{aligned} \tag{40}$$

With $\|\omega_e\|c_1\psi \le \frac{c_1\|\omega_e\|^2\psi_1}{\|\omega_e\|+\varepsilon_3} + \varepsilon_3 c_1\psi_1$ and $\varepsilon_3\psi_1 < \varepsilon_4$, Eq.(40) turns into

$$\begin{aligned}\dot{V}_1 &\le -\chi k_2\omega_e^{\mathrm{T}}\mathrm{sig}^{\alpha}(\omega_e) - \hat{\vartheta}\|\omega-\omega_e\|^2\omega_e^{\mathrm{T}}\tanh(\beta_2\omega_e) \\ &\quad - \frac{\hat{c}_1\|\omega_e\|^2\psi_1}{\|\omega_e\|+\varepsilon_3} + \frac{c_1\|\omega_e\|^2\psi_1}{\|\omega_e\|+\varepsilon_3} + \varepsilon_3 c_1\psi_1 \\ &\quad + \vartheta\|\omega-\omega_e\|^2\|\omega_e\| - \vartheta\|\omega-\omega_e\|^2\omega_e^{\mathrm{T}}\tanh(\beta_2\omega_e) \\ &\quad + \vartheta\|\omega-\omega_e\|^2\omega_e^{\mathrm{T}}\tanh(\beta_2\omega_e) \\ &\quad + \tilde{\vartheta}\|\omega-\omega_e\|^2\omega_e^{\mathrm{T}}\tanh(\beta_2\omega_e) \\ &\quad - b_2\tilde{\theta}^{\mathrm{T}}\hat{\theta} - \beta_3\tilde{\vartheta}\hat{\vartheta} - \frac{\varepsilon_1}{\varepsilon_2}\tilde{c}_1\hat{c}_1 + \frac{\tilde{c}_1\|\omega_e\|^2\psi_1}{\|\omega_e\|+\varepsilon_3} \\ &\le -\chi k_2\omega_e^{\mathrm{T}}\mathrm{sig}^{\alpha}(\omega_e) \\ &\quad + \varepsilon_4 c_1 + \vartheta\|\omega-\omega_e\|^2(\|\omega_e\| - \omega_e^{\mathrm{T}}\tanh(\beta_2\omega_e)) \\ &\quad - b_2\tilde{\theta}^{\mathrm{T}}\hat{\theta} - \beta_3\tilde{\vartheta}\hat{\vartheta} - \frac{\varepsilon_1}{\varepsilon_2}\tilde{c}_1\hat{c}_1\end{aligned} \tag{41}$$

By Lemmas 1 and 2, one has

$$\begin{aligned}\dot{V}_1 &\le -\chi k_2(\omega_e^{\mathrm{T}}\omega_e)^{\frac{1+\alpha}{2}} + \varepsilon_4 c_1 + \frac{3\phi}{\beta_2}\vartheta\|\omega-\omega_e\|^2 \\ &\quad - b_2\tilde{\theta}^{\mathrm{T}}\hat{\theta} - \beta_3\tilde{\vartheta}\hat{\vartheta} - \frac{\varepsilon_1}{\varepsilon_2}\tilde{c}_1\hat{c}_1 \\ &\le -2^{\frac{1+\alpha}{2}}\chi k_2(\frac{1}{2}\omega_e^{\mathrm{T}}\omega_e)^{\frac{1+\alpha}{2}} - (k_1 q_e^{\mathrm{T}}q_e)^{\frac{1+\alpha}{2}} \\ &\quad - (\frac{1}{2b_1}\tilde{\theta}^{\mathrm{T}}\tilde{\theta})^{\frac{1+\alpha}{2}} - (\frac{1}{2\beta_1}\tilde{\vartheta}^2)^{\frac{1+\alpha}{2}} \\ &\quad - (\frac{1}{2\varepsilon_2}\tilde{c}_1^2)^{\frac{1+\alpha}{2}} + (k_1 q_e^{\mathrm{T}}q_e)^{\frac{1+\alpha}{2}} + (\frac{1}{2b_1}\tilde{\theta}^{\mathrm{T}}\tilde{\theta})^{\frac{1+\alpha}{2}} \\ &\quad + (\frac{1}{2\beta_1}\tilde{\vartheta}^2)^{\frac{1+\alpha}{2}} + (\frac{1}{2\varepsilon_2}\tilde{c}_1^2)^{\frac{1+\alpha}{2}} - b_2\tilde{\theta}^{\mathrm{T}}\hat{\theta} - \beta_3\tilde{\vartheta}\hat{\vartheta} \\ &\quad - \frac{\varepsilon_1}{\varepsilon_2}\tilde{c}_1\hat{c}_1 + \varepsilon_4 c_1 + \frac{3\phi}{\beta_2}\vartheta\|\omega_t\|^2 \\ &\le -K_1 V_1^{\frac{1+\alpha}{2}} + (\frac{1}{2b_1}\tilde{\theta}^{\mathrm{T}}\tilde{\theta})^{\frac{1+\alpha}{2}} + (\frac{1}{2\beta_1}\tilde{\vartheta}^2)^{\frac{1+\alpha}{2}} \\ &\quad + (\frac{1}{2\varepsilon_2}\tilde{c}_1^2)^{\frac{1+\alpha}{2}} - b_2\tilde{\theta}^{\mathrm{T}}\hat{\theta} - \beta_3\tilde{\vartheta}\hat{\vartheta} - \frac{\varepsilon_1}{\varepsilon_2}\tilde{c}_1\hat{c}_1 \\ &\quad + \varepsilon_4 c_1 + \frac{3\phi}{\beta_2}\vartheta\|\omega_t\|^2\end{aligned} \tag{42}$$

where $K_1 = \min(2^{\frac{1+\alpha}{2}}\chi k_2, 1)$.

According to

$$\tilde{\theta}^{\mathrm{T}}\hat{\theta} = \frac{1}{2}(\|\tilde{\theta}\|^2 - \|\theta\|^2 + \|\tilde{\theta}+\theta\|^2) \tag{43}$$

$$\tilde{\vartheta}\hat{\vartheta} = \frac{1}{2}(\tilde{\vartheta}^2 - \vartheta^2 + (\tilde{\vartheta}+\vartheta)^2) \tag{44}$$

$$\tilde{c}_1\hat{c}_1 = \frac{1}{2}(\tilde{c}_1^2 - c_1^2 + (\tilde{c}_1+c_1)^2) \tag{45}$$

if $\frac{1}{2b_1}\tilde{\theta}^{\mathrm{T}}\tilde{\theta} > 1$, one has

$$\begin{aligned}(\frac{1}{2b_1}\tilde{\theta}^{\mathrm{T}}\tilde{\theta})^{\frac{1+\alpha}{2}} - b_2\tilde{\theta}^{\mathrm{T}}\hat{\theta} &\le \frac{1}{2b_1}\tilde{\theta}^{\mathrm{T}}\tilde{\theta} - \frac{b_2}{2}\|\tilde{\theta}\|^2 \\ &\quad + \frac{b_2}{2}\|\theta\|^2 - \frac{b_2}{2}\|\tilde{\theta}+\theta\|^2 \\ &\le (\frac{1}{2b_1} - \frac{b_2}{2})\|\tilde{\theta}\|^2 + \frac{b_2}{2}\|\theta\|^2 \\ &\le \frac{b_2}{2}\|\theta\|^2\end{aligned} \tag{46}$$

if $\frac{1}{2b_1}\tilde{\theta}^{\mathrm{T}}\tilde{\theta} \le 1$, one has

$$\begin{aligned}(\frac{1}{2b_1}\tilde{\theta}^{\mathrm{T}}\tilde{\theta})^{\frac{1+\alpha}{2}} - b_2\tilde{\theta}^{\mathrm{T}}\hat{\theta} &\le 1 - \frac{b_2}{2}\|\tilde{\theta}\|^2 \\ &\quad + \frac{b_2}{2}\|\theta\|^2 - \frac{b_2}{2}\|\tilde{\theta}+\theta\|^2 \\ &\le 1 + \frac{b_2}{2}\|\theta\|^2\end{aligned} \tag{47}$$

then,

$$(\frac{1}{2b_1}\tilde{\theta}^{\mathrm{T}}\tilde{\theta})^{\frac{1+\alpha}{2}} - b_2\tilde{\theta}^{\mathrm{T}}\hat{\theta} \le 1 + \frac{b_2}{2}\|\theta\|^2 \tag{48}$$

$$(\frac{1}{2\beta_1}\tilde{\vartheta}^2)^{\frac{1+\alpha}{2}} - \beta_3\tilde{\vartheta}\hat{\vartheta} \le 1 + \frac{\beta_3}{2}\vartheta^2 \tag{49}$$

$$(\frac{1}{2\varepsilon_2}\tilde{c}_1^2)^{\frac{1+\alpha}{2}} - \frac{\varepsilon_1}{\varepsilon_2}\tilde{c}_1\hat{c}_1 \le 1 + \frac{\varepsilon_1}{2\varepsilon_2}c_1^2 \tag{50}$$

With (47)-(50), Eq.(42) can be transformed into

$$\dot{V}_1 \le -K_1 V_1^{\frac{1+\alpha}{2}} + C_1 \tag{51}$$

where $C_1 = \varepsilon_4 c_1 + \frac{3\phi}{\beta_2}\vartheta\|\omega_t\|^2 + 3 + \frac{b_2}{2}\|\theta\|^2 + \frac{\beta_3}{2}\vartheta^2 + \frac{\varepsilon_1}{2\varepsilon_2}c_1^2$.

Step 2. Analyzing the derivative of V_2.

From (20), (22), (26), (28) and (30), it follows that

$$\begin{aligned}\dot{V}_2 &= v_e^{\mathrm{T}} m\dot{v}_e + \rho_1 r_e^{\mathrm{T}}\dot{r}_e + \frac{1}{\delta_1}\tilde{m}\dot{\hat{m}} + \frac{1}{\beta_4}\tilde{\eta}\dot{\hat{\eta}} + \frac{1}{\varepsilon_6}\tilde{c}_2\dot{\hat{c}}_2\\ &= v_e^{\mathrm{T}}(-m\omega^{\times}v_e - m(\omega-\omega_e)^{\times}(\omega-\omega_e)^{\times}Np_t\\ &\quad - mNp_t^{\times}(\omega-\omega_e)^{\times}J_tN^{\mathrm{T}}(\omega-\omega_e) + f + d_f)\\ &\quad + \rho_1 r_e^{\mathrm{T}}(v_e - \omega^{\times}r_e)\\ &\quad + \tilde{m}(-v_e^{\mathrm{T}}(\omega-\omega_e)^{\times}(\omega-\omega_e)^{\times}Np_t - \delta_2\hat{m})\\ &\quad + \tilde{\eta}(\|p_t\|\|\omega-\omega_e\|^2 v_e^{\mathrm{T}}\tanh(\beta_5 v_e) - \beta_6\hat{\eta})\\ &\quad + \frac{1}{\varepsilon_6}\tilde{c}_2(-\varepsilon_5\hat{c}_2 + \frac{\varepsilon_6\|v_e\|^2\psi_2}{\|v_e\|+\varepsilon_7})\\ &= v_e^{\mathrm{T}}(-m(\omega-\omega_e)^{\times}(\omega-\omega_e)^{\times}Np_t\\ &\quad - mNp_t^{\times}(\omega-\omega_e)^{\times}J_tN^{\mathrm{T}}(\omega-\omega_e)\\ &\quad - \rho_1 r_e - k_3\mathrm{sig}^{\alpha}(v_e) - k_4 v_e\\ &\quad + \hat{m}(\omega-\omega_e)^{\times}(\omega-\omega_e)^{\times}Np_t\\ &\quad - \hat{\eta}\|p_t\|\|\omega-\omega_e\|^2\tanh(\beta_5 v_e) - \frac{\hat{c}_2 v_e\psi_2}{\|v_e\|+\varepsilon_7}\\ &\quad + d_f) + \rho_1 r_e^{\mathrm{T}}v_e - \tilde{m}v_e^{\mathrm{T}}(\omega-\omega_e)^{\times}(\omega-\omega_e)^{\times}Np_t\\ &\quad - \delta_2\tilde{m}\hat{m} + \tilde{\eta}\|p_t\|\|\omega-\omega_e\|^2 v_e^{\mathrm{T}}\tanh(\beta_5 v_e)\\ &\quad - \beta_6\tilde{\eta}\hat{\eta} - \frac{\varepsilon_5}{\varepsilon_6}\tilde{c}_2\hat{c}_2 + \frac{\tilde{c}_2\|v_e\|^2\psi_2}{\|v_e\|+\varepsilon_7}\end{aligned}\tag{52}$$

Under Assumption 1 and 2, it shows that

$$\begin{aligned}\dot{V}_2 &\le \|v_e\|m\|J_t\|\|p_t\|\|\omega-\omega_e\|^2 - k_3 v_e^{\mathrm{T}}\mathrm{sig}^{\alpha}(v_e)\\ &\quad - k_4 v_e^{\mathrm{T}}v_e - \hat{\eta}\|p_t\|\|\omega-\omega_e\|^2 v_e^{\mathrm{T}}\tanh(\beta_5 v_e)\\ &\quad - \frac{\hat{c}_2\|v_e\|^2\psi_2}{\|v_e\|+\varepsilon_7} + \|v_e\|c_2\psi_2\\ &\quad - \delta_2\tilde{m}\hat{m} + \tilde{\eta}\|p_t\|\|\omega-\omega_e\|^2 v_e^{\mathrm{T}}\tanh(\beta_5 v_e) - \beta_6\tilde{\eta}\hat{\eta}\\ &\quad - \frac{\varepsilon_5}{\varepsilon_6}\tilde{c}_2\hat{c}_2 + \frac{\tilde{c}_2\|v_e\|^2\psi_2}{\|v_e\|+\varepsilon_7}\end{aligned}\tag{53}$$

By Lemma 1 and using $\eta = m\|J_t\|$, $\|v_e\|c_2\psi_2 \le \frac{c_2\|v_e\|^2\psi_2}{\|v_e\|+\varepsilon_7} + \varepsilon_7 c_2\psi_2$ and $\varepsilon_7\psi_2 < \varepsilon_8$, it follows that

$$\begin{aligned}\dot{V}_2 &\le -k_3(v_e^{\mathrm{T}}v_e)^{\frac{1+\alpha}{2}} + \eta\|p_t\|\|\omega-\omega_e\|^2(\|v_e\|\\ &\quad - v_e^{\mathrm{T}}\tanh(\beta_5 v_e)) - \frac{\tilde{c}_2\|v_e\|^2\psi_2}{\|v_e\|+\varepsilon_7} + \varepsilon_8 c_2\\ &\quad - \tilde{\eta}\|p_t\|\|\omega-\omega_e\|^2 v_e^{\mathrm{T}}\tanh(\beta_5 v_e) - \delta_2\tilde{m}\hat{m}\\ &\quad + \tilde{\eta}\|p_t\|\|\omega-\omega_e\|^2 v_e^{\mathrm{T}}\tanh(\beta_5 v_e)\\ &\quad - \beta_6\tilde{\eta}\hat{\eta} - \frac{\varepsilon_5}{\varepsilon_6}\tilde{c}_2\hat{c}_2 + \frac{\tilde{c}_2\|v_e\|^2\psi_2}{\|v_e\|+\varepsilon_7}\\ &\le -k_3(v_e^{\mathrm{T}}v_e)^{\frac{1+\alpha}{2}} + \eta\|p_t\|\|\omega-\omega_e\|^2(\|v_e\|\\ &\quad - v_e^{\mathrm{T}}\tanh(\beta_5 v_e)) + \varepsilon_8 c_2 - \delta_2\tilde{m}\hat{m}\\ &\quad - \beta_6\tilde{\eta}\hat{\eta} - \frac{\varepsilon_5}{\varepsilon_6}\tilde{c}_2\hat{c}_2\end{aligned}\tag{54}$$

With Lemmas 1 and 2, Eq.(54) can be expressed as

$$\begin{aligned}\dot{V}_2 &\le -K_2 V_2^{\frac{1+\alpha}{2}} + \frac{3\phi}{\beta_5}\eta\|p_t\|\|\omega_t\|^2\\ &\quad + \varepsilon_8 c_2 + (\frac{\rho_1}{2}r_e^{\mathrm{T}}r_e)^{\frac{1+\alpha}{2}} + (\frac{1}{2\delta_1}\tilde{m}^2)^{\frac{1+\alpha}{2}}\\ &\quad + (\frac{1}{2\beta_4}\tilde{\eta}^2)^{\frac{1+\alpha}{2}} + (\frac{1}{2\varepsilon_6}\tilde{c}_2^2)^{\frac{1+\alpha}{2}} - \delta_2\tilde{m}\hat{m}\\ &\quad - \beta_6\tilde{\eta}\hat{\eta} - \frac{\varepsilon_5}{\varepsilon_6}\tilde{c}_2\hat{c}_2\end{aligned}\tag{55}$$

where $K_2 = \min(2^{\frac{1+\alpha}{2}}k_3, 1)$.

With the similar analyzing procedure of Eqs.(43)-(50), it follows that

$$(\frac{1}{2\delta_1}\tilde{m}^2)^{\frac{1+\alpha}{2}} - \delta_2\tilde{m}\hat{m} \le 1 + \frac{\delta_2}{2}m^2 \tag{56}$$

$$(\frac{1}{2\beta_4}\tilde{\eta}^2)^{\frac{1+\alpha}{2}} - \beta_6\tilde{\eta}\hat{\eta} \le 1 + \frac{\beta_6}{2}\eta^2 \tag{57}$$

$$(\frac{1}{2\varepsilon_6}\tilde{c}_2^2)^{\frac{1+\alpha}{2}} - \frac{\varepsilon_5}{\varepsilon_6}\tilde{c}_2\hat{c}_2 \le 1 + \frac{\varepsilon_5}{2\varepsilon_6}c_2^2 \tag{58}$$

Thus,

$$\begin{aligned}\dot{V}_2 &\le -K_2 V_2^{\frac{1+\alpha}{2}} + \frac{3\phi}{\beta_5}\eta\|p_t\|\|\omega_t\|^2 + \varepsilon_8 c_2\\ &\quad + (\frac{\rho_1}{2}r_e^{\mathrm{T}}r_e)^{\frac{1+\alpha}{2}} + 3 + \frac{\delta_2}{2}m^2 + \frac{\beta_6}{2}\eta^2 + \frac{\varepsilon_5}{2\varepsilon_6}c_2^2\\ &\le -K_2 V_2^{\frac{1+\alpha}{2}} + C_2\end{aligned}\tag{59}$$

where $C_2 = \frac{3\phi}{\beta_5}\eta\|p_t\|\|\omega_t\|^2 + \varepsilon_8 c_2 + (\frac{\rho_1}{2}r_e^{\mathrm{T}}r_e)^{\frac{1+\alpha}{2}} + 3 + \frac{\delta_2}{2}m^2 + \frac{\beta_6}{2}\eta^2 + \frac{\varepsilon_5}{2\varepsilon_6}c_2^2$.

Step 3. Analyzing the derivative of V.

From Eqs.(32), (51) and (59), one has

$$\begin{aligned}\dot{V} &= \dot{V}_1 + \dot{V}_2\\ &\le -K_1 V_1^{\frac{1+\alpha}{2}} + C_1 - K_2 V_2^{\frac{1+\alpha}{2}} + C_2\\ &\le -KV^{\frac{1+\alpha}{2}} + C\end{aligned}\tag{60}$$

where $K = \min(K_1, K_2)$, $C = C_1 + C_2$.

By Lemma 3, the coupling relative motion system (19)-(22) with 6-DOF controller (23)-(24) is practical FT stable, i.e. the control objective can be realized.

Remark 2 The adaptive update laws (25)-(30) are constructed to accurately compensate the effect of the unknown terms included the uncertain inertia and mass and unknown time-varying state-dependent disturbance.

Remark 3 From the analysis of the theorem 1, the proposed 6-DOF adaptive finite-time control laws (23)-(24) can also accomplish the FT convergence of the system (19)-(22) with the state-independent disturbances bounded by unknown constants.

4. NUMERICAL SIMULATION

To show the performance and superiorities of the proposed coupled AFT 6-DOF tracking controller, numerous comparison simulations are studied. The initial state values are given in Table 1.

Table 1. Initial state values

State variables	Initial values
r	$[10, 10, 10]^{\mathrm{T}}$ m
v	$[0, 0, 0]^{\mathrm{T}}$ m/s
$[q^{\mathrm{T}}, \varsigma]^{\mathrm{T}}$	$[0.06, 0.69, 0.06, -0.72]^{\mathrm{T}}$
ω	$[0, 0, 0]^{\mathrm{T}}$ rad/s
r_t	$[3, 3, 3]^{\mathrm{T}}$ m
v_t	$[0, 0, 0]^{\mathrm{T}}$ m/s
$[q_t^{\mathrm{T}}, \varsigma_t]^{\mathrm{T}}$	$[0.2, 0.1, 0.3, -0.93]^{\mathrm{T}}$
ω_t	$[0.2, 0.2, 0.2]^{\mathrm{T}}$ rad/s

The following physical variables are selected as $m = 200$ kg, $J = \begin{bmatrix} 75.0 & -28.1 & -28.1 \\ -28.1 & 75.0 & -28.1 \\ -28.1 & -28.1 & 75.0 \end{bmatrix}$ kgm^2, $m_t = 300$ kg, $p_t = [0, 5, 0]^{\mathrm{T}}$m, $J_t = \begin{bmatrix} 50 & 0 & 0 \\ 0 & 275 & 0 \\ 0 & 0 & 275 \end{bmatrix}$ kgm^2.

In addition, the parameters of the proposed AFT 6-DOF controller and the designed adaptive update laws are set as $k_1 = 700$, $\sigma_1 = 0.03$, $\sigma_2 = 0.1$, $k_2 = 300$, $k_3 = 500$, $k_4 = 500$, $\rho_1 = 500$, $\alpha = 3/5$, $\delta_1 = 100$, $\delta_2 = 10$, $b_1 = 1$, $b_2 = 1$, $\beta_1 = 0.5$, $\beta_2 = 10$, $\beta_3 = 20$, $\beta_4 = 0.5$, $\beta_5 = 500$, $\beta_6 = 10$, $\varepsilon_1 = 1000$, $\varepsilon_2 = 500$, $\varepsilon_4 = 0.5$, $\varepsilon_5 = 1000$, $\varepsilon_6 = 500$, $\varepsilon_8 = 0.5$. The initial variables $\hat{\theta}(0) = [0; 0; 0; 0; 0; 0]$, $\hat{m}_1(0) = 0$, $\hat{\vartheta}_1(0) = 0$, $\hat{\eta}_1(0) = 0$, $\hat{c}_1(0) = 0$ and $\hat{c}_2(0) = 0$.

The advantages of the AFT 6-DOF controller (23,24) is illustrated by compared with the PD-type $H\infty$ controller (Kasiri and Fani Saberi (2023)) $f = -\frac{1}{a_2}(k_{p1} r_e + K_{d1} v_e)$ and $\tau = -\frac{1}{b_3}(K_{q_e} q_e + K_{d2}\omega_e)$, where $a_2 = b_3 = 1$, $k_{p1} = 500 I_3$, $K_{d1} = 500 I_3$, $K_{q_e} = (\varsigma_e I_3 - q_e^{\times}) K_{p2} + k_{p3}(1 - \varsigma_e) I_3$, $K_{p2} = 700 I_3$, $k_{p3} = 50$ and $K_{d2} = 300 I_3$.

Case 1. For spacecraft state-dependent disturbances $d_f = (1 + \|v\|^2)[0.2\cos(t), 0.5\sin(t), 0.3\sin(t)]^{\mathrm{T}}$ N and $d_\tau = (1 + \|\omega\|^2)[0.2\cos(t), 0.5\sin(t), 0.3\sin(t)]^{\mathrm{T}}$ N·m, the system state tracking error curves are shown in Figs. 3-6 under the AFT 6-DOF controller (23,24) and the PD-type $H\infty$ controller.

Fig. 3 depicts the attitude errors. The absolute values of attitude tracking error $q_e(i)$ under the AFT 6-DOF controller and the PD-type $H\infty$ controller converge to less than 5×10^{-3} at 11s and 9×10^{-3} at 23s, respectively, where $q_e(i)$ denotes the ith elements of the vector q_e. Fig. 4 gives the angular errors. The absolute values of $\omega_e(i)$ using the AFT 6-DOF controller and the PD-type $H\infty$ controller converge to less than 2×10^{-3} rad/s at 16s and 5×10^{-3} rad/s at 18s, respectively, where $\omega_e(i)$ denotes the ith elements of ω_e. Figs. 5 and 6 plot the position errors and velocity errors, respectively. Using the proposed controller, the absolute values of $r_e(i)$ and $v_e(i)$ converge to less than 0.09 m and 0.05 m/s at 12s and 13s, respectively. Meanwhile, using the PD-type $H\infty$ controller, the absolute values of $r_e(i)$ and $v_e(i)$ converge to less than 0.30 m and 0.20 m/s at 15s and 14s, respectively. $r_e(i)$ and $v_e(i)$ denote the ith elements of r_e and v_e, respectively. Table 2 detailed describe the convergence time and control precision with $i = 1, 2, 3$ for Case 1, which shows that the AFT 6-DOF controller provides higher control performance.

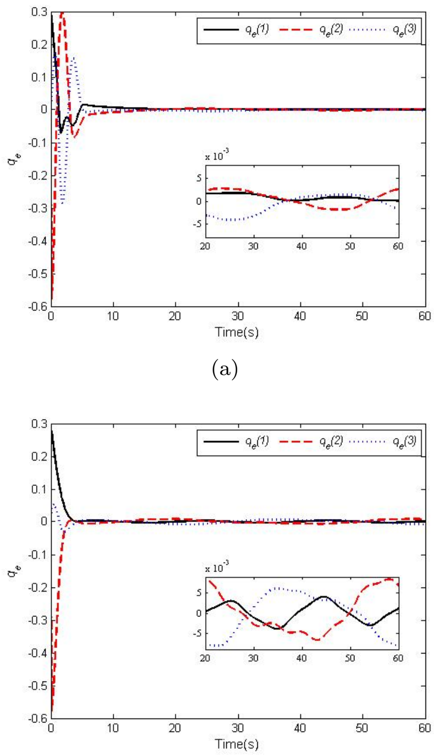

(a)

(b)

Fig. 3. q_e using the AFT 6-DOF (a) and PD-type $H\infty$ (b) controllers.

Case 2. For state-independent disturbances with big upper bounds $d_f = [1.5\cos(t), 2.5\sin(t), 1.5\sin(t)]^{\mathrm{T}}$ N and $d_\tau = [1.0\cos(t), 2.5\sin(t), 1.5\sin(t)]^{\mathrm{T}}$ N·m, the response errors are depicted in Figs. 7-10.

Fig. 7 gives the attitude tracking error curves and Fig. 8 depicts the angular tracking error curves. The up bounds of the errors of Figs. 7(a) and 8(a) are 5×10^{-3} at 12s and 2×10^{-3} at 16s, but the up bounds of the errors of Figs. 7(b) and 8(b) are 0.01 at 22s and 9×10^{-3} at 18s. Figs. 9 and 10 plot the curves of position tracking and velocity tracking, respectively. It can be seen that the error bounds of Figs. 9(a) and 10(a) are 0.09 at 11s and 0.05 at 13s, while the error bounds of Figs. 9(b) and 10(b) are 0.30 at 12s and 0.12 at 18s. Using the AFT 6-DOF controller and the PD-type $H\infty$ controller, table 3 with $i = 1, 2, 3$ gives the convergence time and control precision for Case 2. Table 3 shows that the AFT 6-DOF controller provides higher control performance.

Table 2. Convergence time and control precision for Case 1.

Tracking error	AFT 6-DOF controller		PD-type $H\infty$ controller	
	time(s)	**precision**	**time(s)**	**precision**
$\lvert q_e(i)\rvert$	11	5×10^{-3}	23	9×10^{-3}
$\lvert \omega_e(i)\rvert$	16	2×10^{-3}	18	5×10^{-3}
$\lvert r_e(i)\rvert$	12	0.09	15	0.30
$\lvert v_e(i)\rvert$	13	0.05	14	0.20

Table 3. Convergence time and control precision for Case 2.

Tracking error	AFT 6-DOF controller		PD-type $H\infty$ controller	
	time(s)	**precision**	**time(s)**	**precision**
$\lvert q_e(i)\rvert$	12	5×10^{-3}	22	0.01
$\lvert \omega_e(i)\rvert$	16	2×10^{-3}	18	9×10^{-3}
$\lvert r_e(i)\rvert$	11	0.09	12	0.30
$\lvert v_e(i)\rvert$	13	0.05	18	0.12

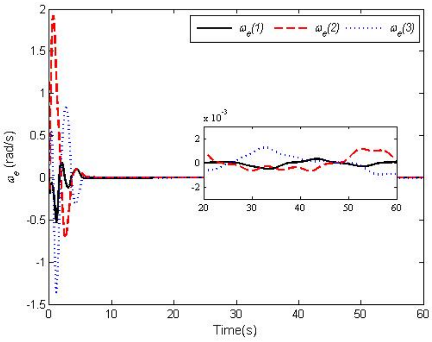

(a)

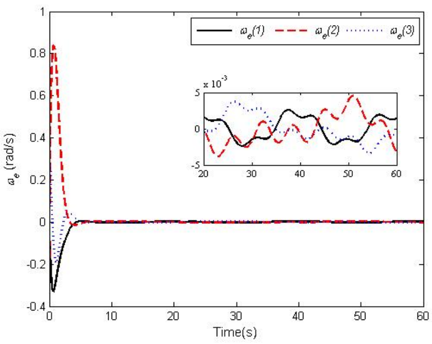

(b)

Fig. 4. ω_e using the AFT 6-DOF (a) and PD-type $H\infty$ (b) controllers.

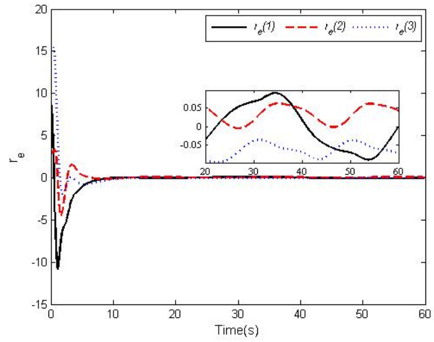

(a)

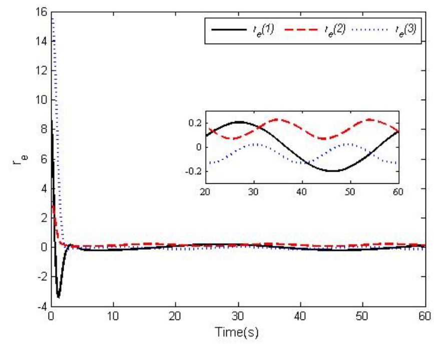

(b)

Fig. 5. r_e using the AFT 6-DOF (a) and PD-type $H\infty$ (b) controllers.

From Figs. 3-10 for satellite under Case 1 and Case 2, the tracking error curves are smooth, i.e. the system geometric singularity is avoided, and the influence of the unknown uncertainties and the unknown time-varying disturbances can be restrained accurately by compared with the PD-type $H\infty$ controller. Combining Lemma 3 and Remark 3, the proposed coupled AFT 6-DOF tracking controller can implement the finite time stability instead of bounded or asymptotic stability.

Considering the Case 1 and Case 2 and to analyse Figs. 3-10 and Tables 2 and 3, the advantages of the proposed AFT 6-DOF control algorithm are very obvious and it can be observed as follows: 1) The absolute values of attitude tracking error $q_e(i)$ with the AFT 6-DOF controller and the PD-type $H\infty$ controller can converge to less than 5×10^{-3} at 12s and 0.01 at 23s, respectively. 2) The absolute values of $\omega_e(i)$ using the AFT 6-DOF controller and the PD-type $H\infty$ controller converge to less than 2×10^{-3} rad/s at 16s and 9×10^{-3} rad/s at 18s, respectively. 3) Using the proposed controller, the absolute values of $r_e(i)$ and $v_e(i)$ converge to less than 0.09 m and 0.05 m/s at 12s and 13s, respectively. Meanwhile, using the PD-type $H\infty$ controller, the absolute values of $r_e(i)$ and $v_e(i)$ converge to less than 0.30 m and 0.20 m/s at 15s and 18s, respectively. Thus, the proposed coupled AFT 6-DOF tracking controller can implement the faster convergence and better robustness by compared withthe PD-type $H\infty$ controller.

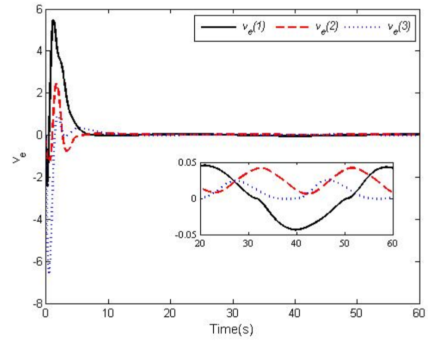

(a)

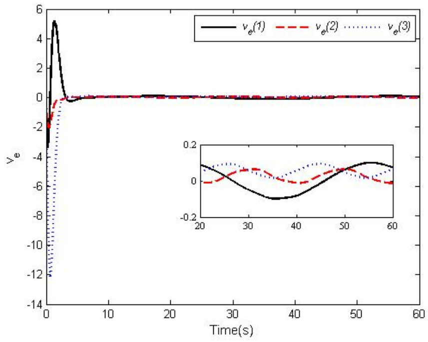

(b)

Fig. 6. v_e using the AFT 6-DOF (a) and PD-type $H\infty$ (b) controllers.

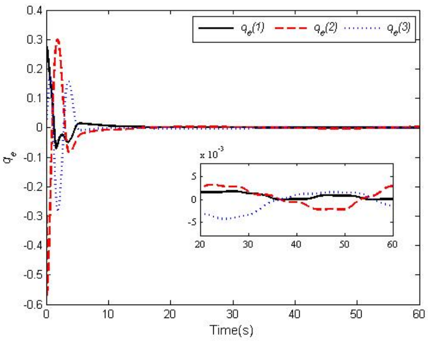

(a)

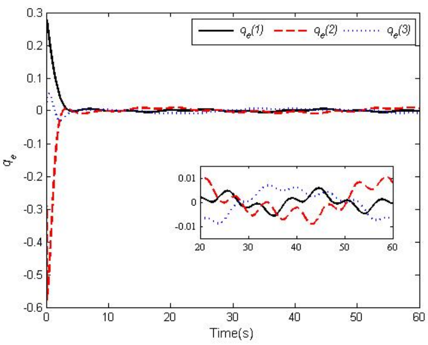

(b)

Fig. 7. q_e using the AFT 6-DOF (a) and PD-type $H\infty$ (b) controllers.

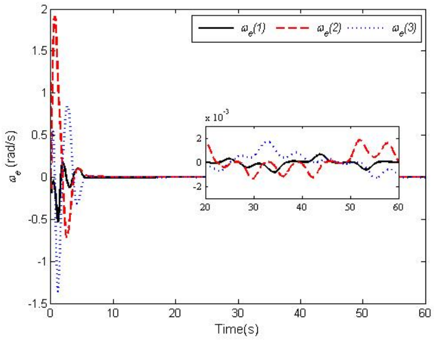

(a)

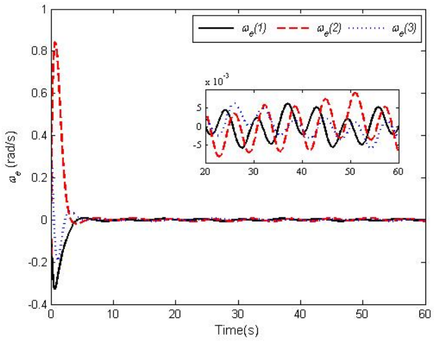

(b)

Fig. 8. ω_e using the AFT 6-DOF (a) and PD-type $H\infty$ (b) controllers.

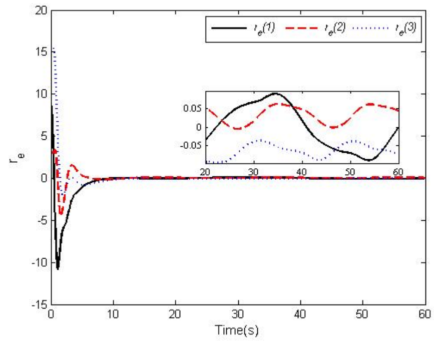

(a)

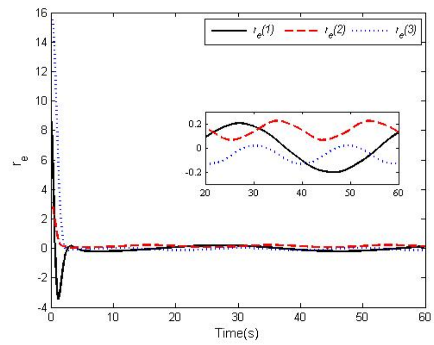

(b)

Fig. 9. r_e using the AFT 6-DOF (a) and PD-type $H\infty$ (b) controllers.

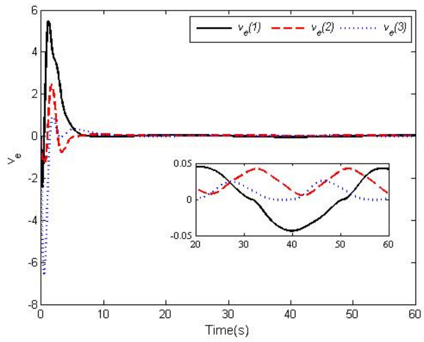

(a)

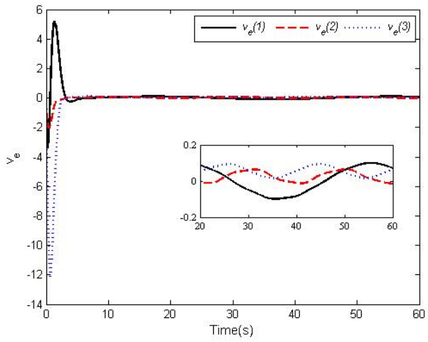

(b)

Fig. 10. v_e using the AFT 6-DOF (a) and PD-type $H\infty$ (b) controllers.

5. CONCLUSION

In this study, for satellite proximation operations with non-cooperative target, uncertain mass and inertia and state-dependent disturbance, an AFT 6-DOF control problem of the pursuing satellite is studied. The coupled dynamics of relative motion are modeled with consider of the coupling. An AFT 6-DOF coupled control strategy with a self-adjustment function is constructed to realize a good control performance. The comparison of simulation results show that the AFT 6-DOF control scheme has nice convergence rate and precision.

REFERENCES

Chen, L., Sun, Y., Shao, X., Chen, J., and Zhang, D. (2023). Adaptive prescribed-time control for coupled 6-dof spacecraft formation flying. *International Journal of Control, Automation and Systems*, 21(2), 350–358.

Hardy, G.H., Littlewood, J.E., and Pólya, G. (1952). *Inequalities.* Cambridge university press.

Kasiri, A. and Fani Saberi, F. (2023). Coupled position and attitude control of a servicer spacecraft in rendezvous with an orbiting target. *Scientific Reports*, 13(1), 4182.

Lee, D. and Gallucci, S. (2023). Spacecraft attitude estimation under attitude tracking maneuver during close-proximity operations. *Advances in Space Research*, 71(10), 4315–4331.

Li, Q., Yuan, J., Zhang, B., and Wang, H. (2018). Disturbance observer based control for spacecraft proximity operations with path constraint. *Aerospace Science and Technology*, 79, 154–163.

Liu, K., Wang, Y., Ji, H., and Wang, S. (2021). Adaptive saturated tracking control for spacecraft proximity operations via integral terminal sliding mode technique. *International Journal of Robust and Nonlinear Control*, 31(18), 9372–9396.

Oestreich, C.E., Linares, R., and Gondhalekar, R. (2021). Autonomous six-degree-of-freedom spacecraft docking with rotating targets via reinforcement learning. *Journal of Aerospace Information Systems*, 18(7), 417–428.

POLYCARPOU, M. and IOANNOU, P. (1996). A robust adaptive nonlinear control design. *Automatica (Oxford)*, 32(3), 423–427.

Shao, X., Hu, Q., and Shi, Y. (2020). Adaptive pose control for spacecraft proximity operations with prescribed performance under spatial motion constraints. *IEEE Transactions on Control Systems Technology*, 29(4), 1405–1419.

Sun, L. and Huo, W. (2014). Nonlinear robust adaptive control for spacecraft proximity operations. *IFAC Proceedings Volumes*, 47(3), 2219–2224.

Wang, G., Liu, K., Sun, Z., and Li, Y. (2020). Attitude-orbit cooperative control for small-scale spacecraft with chemical propulsion: Adaptive sliding mode control based on neural network. *Journal of Aerospace Engineering*, 33(6), 04020080.

Wang, L., Guo, Y., Ma, G., and Zhang, H. (2022). Artificial potential function based spacecraft proximity maneuver 6-dof control under multiple pyramid-type constraints. *ISA transactions*, 126, 316–325.

Wang, W., Li, C., and Guo, Y. (2021). Relative position coordinated control for spacecraft formation flying with obstacle/collision avoidance. *Nonlinear Dynamics*, 104, 1329–1342.

Zhang, Y., Wu, G., Yang, X., and Song, S. (2022). Appointed-time prescribed performance control for 6-dof spacecraft rendezvous and docking operations under input saturation. *Aerospace Science and Technology*, 128, 107744.

Zhao, Q. and Duan, G. (2023). Prescribed performance tracking control for spacecraft proximity operations with inertia property identification. *Aerospace Science and Technology*, 141, 108555.

Zhu, Z., Xia, Y., and Fu, M. (2011). Attitude stabilization of rigid spacecraft with finite-time convergence. *International Journal of Robust and Nonlinear Control*, 21(6), 686–702.

Zhu, Z., Gao, Z., and Guo, Y. (2024). Backstepping-based six degrees of freedom adaptive control for spacecraft tracking a noncooperative target. *Journal of Circuits, Systems and Computers*, 33(01), 2450004.

Zhu, Z., Guo, Y., and Gao, Z. (2020). Distributed coordinated attitude regulation control for multiple spacecraft with time-varying uncertainties. *Journal of Circuits, Systems and Computers*, 29(01), 2050018.

Zhuang, M., Liguo, T., Kehang, L., and Shenmin, S. (2021). Fixed-time position coordinated tracking control for spacecraft formation flying with collision avoidance. *Chinese Journal of Aeronautics*, 34(11), 182–199.